

Development of pre-processing techniques for the new 30 THz infrared telescope

F. Manini[1,2], C. Francile[1,2], F.M. López[1,3], R.F. Hidalgo Ramirez[4], A.S. Kudaka[4] & J.P. Raulin[4]

[1] *Facultad de Ciencias Exactas, Físicas y Naturales, UNSJ, Argentina.*
[2] *Observatorio Astronómico Félix Aguilar, UNSJ, Argentina*
[3] *Instituto de Ciencias Astronómicas, de la Tierra y del Espacio, CONICET–UNSJ, Argentina.*
[4] *Centro de Rádio Astronomia e Astrofísica Mackenzie, Universidade Presbiteriana Mackenzie, São Pablo, Brasil*

Contact / francoamaninig@gmail.com

Resumen / En el presente trabajo se reporta el desarrollo de técnicas de preprocesamiento de imágenes para el nuevo telescopio solar de 30 THz ubicado en la Estación Astronómica C. Cesco, El Leoncito, San Juan, Argentina. Esto incluye: corrección por campo plano, corrección por oscurecimiento al limbo, centrado y rotación de las imágenes respecto al norte solar, creación del encabezado para cada archivo de imágen bajo estándares Solar SoftWare (SSW), salida en formato estándar FITS y la automatización de los procesos anteriores, con la creación de una interfaz gráfica. Esto será usado para investigar fenómenos solares transitorios en esta banda asociados a regiones activas y estructuras fotosféricas tales como manchas solares y plages.

Abstract / In this work we report on the development of image pre-processing techniques for the new 30 THz solar telescope located in the Estación Astronómica C. Cesco, El Leoncito, San Juan, Argentina. This includes: flat fielding correction, limb darkening correction, centering and north rotation of the images, header creation for each image under Solar SoftWare (SSW) standards, FITS standard format for the output images and automation of the processes, also with the creation of a graphic user interface. These data will be used to study transitory solar phenomena associated with active regions and photospheric structures such as sunspots and plagues.

Keywords / Sun: photosphere — Sun: infrared — Methods: observational

1. Introduction

A new 20 cm infrared telescope was recently installed in the Estación Astronómica C. Cesco for solar photospheric observations at 30 THz (10 μm). The investigation of the Sun in this region of the spectrum is in growing development due to the rise of new technologies in cameras and detectors. This telescope has an infrared camera which is ideal to study sunspots evolution, plages and transient events such as flares. Since this is a new instrument, a pre-processing routine package is not available yet for flat-field correction, limb darkening, image registration (centering and image orientation), and generation of FITS (Flexible Image Transport System) standard format files, with heading under Solar SoftWare (SSW) standards. Because of this, the development of pre-processing techniques for the images acquired with the camera is of fundamental interest to improve the scientific study of the Sun in this region of the spectrum.

Technical details about the instrument can be found in Manini et al. (2017). One of the events that we use in this report occurred on September 4th, 2017, when two active regions were present: AR12673 (north) and AR12674 (south). We will use these images to show how we apply the pre-processing routines and how sunspots are seen in infrared.

2. Pre-processing techniques

Once the raw images have been acquired and saved in Flir Public Format (FPF), which is the proprietary format of the camera, we can start with the following preprocessing steps:

2.1. Flat-field correction

The fact that there are no extended and homogeneous radiation sources similar in intensity to the Sun, and with temperatures like those found on the Solar photosphere (4000-6000 K), requires the implementation of synthetic methods to obtain flat-field images. In this work we applied a process that creates a flat mask for the 30 THz camera using the method developed by Kuhn et al. (1991).

The process to obtain the images begins when the operator of the telescope gets the images which are going to be used to construct the flat image. For this, the operator moves the solar disk over the camera frame in a random manner with the manual control while approximately 200 images are taken. 100 of them will be randomly selected to perform the flat-fielding process. This quantities were determined empirically, given that with a higher or lower amount, the result worsen. The process needs to be done in favorable conditions (no clouds near the Sun, and no solar activity, if possible).

Once the FPF images are saved, the flat creation process begins, with an IDL routine which applies the method developed by Kuhn et al. (1991) described below:

To begin with, the routine creates a circular mask with a radius of 330 pixels that is used to eliminate the edges of the image, i.e leave the solar limb outside (because of its high intensity gradient which introduces spurious values in the algorithm). Then 100 images are randomly selected from the total set. After that, it begins to iterate, reading the offset from the solar disk center respect to the center of the image. The *roberts* filter (Davis, 1975) is used, which is a function that returns the approximate value of the Roberts operator, that serves to highlight the edges.

The routine then finds the pixels that define the solar limb, and generates an array where the limb is defined. Then a circumference is interpolated to the limb position with the *mpfit* package (Markwardt, 2009), this function returns an array with the parameters of the circumference, in our case, the x-y position of the center and the radius. In the set of images, it saves the central sector of the selected image using the mask.

Being the image set defined with its respective centers, the routine creates the flat, using the function *mk kuhn flat* from SSW. It requires the spatially displaced set of images previously found, and a threshold value, over which the image data and the iteration number are considered valid. Empirically, a threshold of 0.1 and an iteration number of 10 are used to get a good results. It was determined that applying the process for a second time to the flat corrected images considerably improves the results, for which the final flat image is obtained as $flat = flat_{step1} * flat_{step2}$. This method assumes that the source (Sun) does not change between frames, thus the signal observed in an image i in a pixel x can be expressed as:

$$D_i(x) = G(x)S_i(x), \tag{1}$$

where $G(x)$ is the detector gain and $S(x)$ the source. A detector gain matrix can be built from misaligned images i,j from the Sun, by minimizing the expression:

$$\sum_{i>j,x} [D_i(x+a_i)-D_j(x+a_j)-G(x+a_i)+G(x+a_j)]^2, \tag{2}$$

with a_i, a_j being the displacement vectors. Kuhn et al. (1991) developed an iterative algorithm to calculate the gain mask of the array as follows:

$$G^{r+1}(x) = K(x)\frac{1}{n(x)}\sum_{i<j}[G^r(x-a_i+a_j)+ G^r(x-a_j+a_i)], \tag{3}$$

where

$$K(x) = \frac{1}{n(x)}\sum_{i<j}[D_i(x)-D_j(x-a_i+a_j)]+ [D_j(x)-D_i(x-a_j+a_i)]. \tag{4}$$

This way, through successive iterations, and considering the threshold level, a gain mask of sufficient precision is obtained. Then, the images are corrected by dividing each raw image by the created flat. The results of the application of this method are shown in Fig. 1.

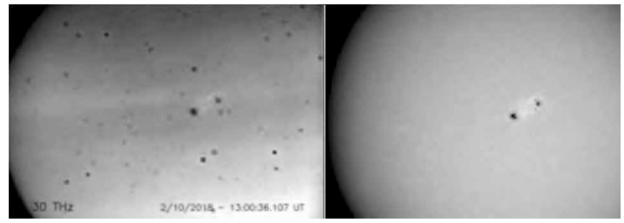

Figure 1: 30 THz image from February 10th, 2018. Left: No flat fielding is applied, tiny black dots are seen on the image, which are produced by dust particles over the camera. Right: Once the flat fielding is applied, the dust is removed and two sunspots are clearly visible.

2.2. Image registration: Centering and orientation of the images

Image registration consists of two steps: one is centering the image, which means to match the center of the Sun with the central pixel of the image frame; the other is rotation, which brings the solar north upwards aligned with the vertical axis of the frame, and the solar west to the rightmost of the frame (Thompson, 2006). This serves as a reference for the final user. The first step in this process is to open the flat corrected image, and through the *sxpar* function, extract from the header the x and y coordinates of the solar rotational axis in the ecliptic coordinates system, the position angle of the solar center, $P0$, and the measured deviation angle of the camera, of -15.574 °, taken from Manini et al. (2017). The original size of the frame is 640x480 pixels^2, and the pixel whose coordinates are (0,0) in IDL, is located on the lower left corner of it. The full solar disk does not fit in in a frame, the solar radius of 15.994 arcmin and a pixel scale of 2.55 arcsec obtained for the observation (Manini et al., 2017) results in a solar radius of 376 pixels.

The process continues by reversing the image horizontally, so as to leave the west to the right of the frame, using the function *reverse*. This is due to the image reflection in a mirror situated in front of the camera. Then, the array containing the frame is enlarged to 1280x960 pixels^2, because when performing the rotation, some portions of the solar disk might be lost. The displacement of the image is done, placing the center of the Sun in the center of the new frame, and then the image is rotated with the function *rot*, which needs the rotation angle (clock-wards), defined as the sum of the deviation angle of the camera and the position angle $P0$, as well as the position of the pixel that defines the center of rotation. The function uses a cubic interpolation approach.

2.3. Limb darkening correction

The method to correct the images by limb darkening was previously published in Manini et al. (2017). The results of the method can be seen in Fig. 3.

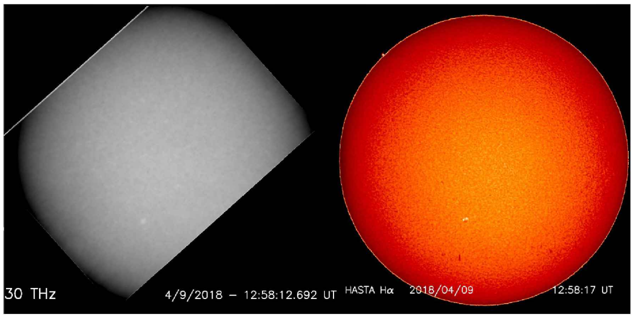

Figure 2: To the left: 30 THz rotated image. To the right: H_α image obtained by the HASTA telescope. Both images are centered, with the solar north upwards, and were taken on April 8th, 2018. In both pictures a small plage is observed.

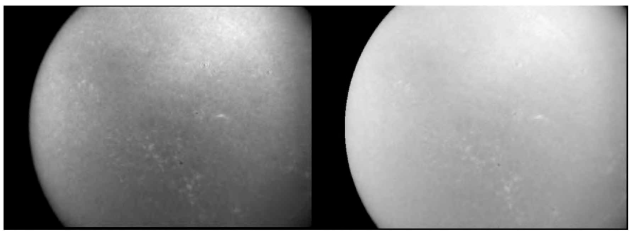

Figure 3: Limb darkening correction. Left: Raw 30 THz image without correction. Right: Same image corrected by limb darkening with the method by Manini et al. (2017). The image was acquired on May 21st, 2017.

2.4. Output in FITS standard format and automation of the processes.

All previous routines were automated in order to simplify the process. An IDL program was created, which selects the FPF images of the day from a specified folder and then performs the flat correction for this set of images, with an option to convert to FITS format. Once the image format is selected, its up to the operator's choice whether to correct the images by limb darkening using the method previously mentioned, and to rotate them. At the same time, a header is created for each image using the routine *mkhdr* where some parameters are added using the *sxaddpar* function, having almost 70 parameters for each image. This was made taking into account the SSW standards (S.L.Freeland, 1999; Hanisch et al., 2001).

3. Results and conclusions

In Fig. 4 the full pre-processing applied to a 30 THz image taken on September 4th, 2017 where two group of sunspots are seen. To compare and verify the accuracy of the results, we show a continuum image from the *Solar Dynamic Observatory (SDO)*. A graphic user interface is being developed, in which all the routines are automated to simplify the user operation.

The proposed preprocessing method has proven to be accurate, as it has also been tested with images taken in different times of the year, and compared with calibrated images from several telescopes. So, it is an easy, fast and practical way for the user to pre-process the images taken with this instrument. Given that the telescope is new, the preprocessed images are now ready to be used to provide new insights for the Sun at this wavelength.

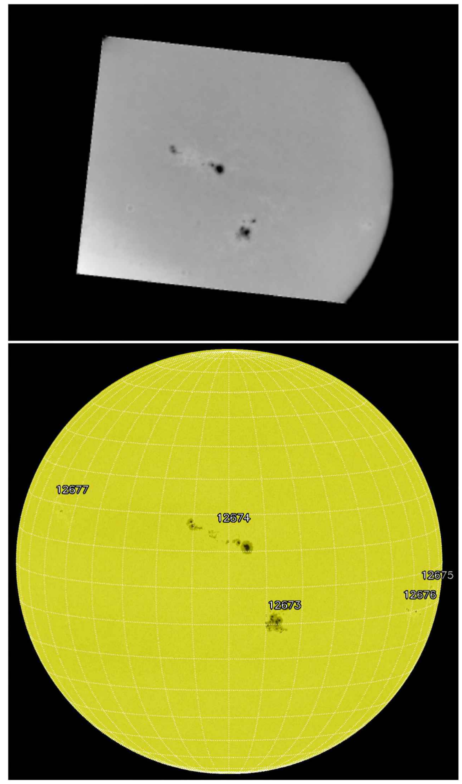

Figure 4: Upper panel: Final image obtained in 10 μm after the application of our pre-processing methodology. Lower panel: A 617,3 nm solar image obtained by *HMI/SDO*. Image from www.solarmonitor.org. Both images correspond to September 4th, 2017.

References

Davis L., 1975, Computer Graphics and Image Processing, 4, 248

Hanisch R.J., et al., 2001, Astronomy and Astrophysics, 376, 359

Kuhn J., Lin H., Loranz D., 1991, Publications of the astronomical society of the pacific, 103, 1097

Manini F., et al., 2017, BAAA

Markwardt C., 2009, D. Bohlender, D. Durand, P. Dowler (Eds.), *Astronomical Data Analysis Software and Systems XVIII, Astronomical Society of the Pacific Conference Series*, vol. 411, 251

S.L.Freeland, 1999, *SSW Keyword/Tag Definitions*

Thompson W.T., 2006, Astronomy and Astrophysics, 449, 791